Microstructural visual system changes in AQP4-antibody–seropositive NMOSD

OPEN

Frederike C. Oertel*
Joseph Kuchling, MD*
Hanna Zimmermann, MEng
Claudia Chien, MSc
Felix Schmidt, MD
Benjamin Knier, MD
Judith Bellmann-Strobl, MD
Thomas Korn, MD
Michael Scheel, MD
Alexander Klistorner, MD
Klemens Ruprecht, MD
Friedemann Paul, MD
Alexander U. Brandt, MD

Correspondence to
Dr. Brandt:
alexander.brandt@charite.de

ABSTRACT

Objective: To trace microstructural changes in patients with aquaporin-4 antibody (AQP4-ab)-seropositive neuromyelitis optica spectrum disorders (NMOSDs) by investigating the afferent visual system in patients without clinically overt visual symptoms or visual pathway lesions.

Methods: Of 51 screened patients with NMOSD from a longitudinal observational cohort study, we compared 6 AQP4-ab–seropositive NMOSD patients with longitudinally extensive transverse myelitis (LETM) but no history of optic neuritis (ON) or other bout (NMOSD-LETM) to 19 AQP4-ab–seropositive NMOSD patients with previous ON (NMOSD-ON) and 26 healthy controls (HCs). Foveal thickness (FT), peripapillary retinal nerve fiber layer (pRNFL) thickness, and ganglion cell and inner plexiform layer (GCIPL) thickness were measured with optical coherence tomography (OCT). Microstructural changes in the optic radiation (OR) were investigated using diffusion tensor imaging (DTI). Visual function was determined by high-contrast visual acuity (VA). OCT results were confirmed in a second independent cohort.

Results: FT was reduced in both patients with NMOSD-LETM ($p = 3.52e^{-14}$) and NMOSD-ON ($p = 1.24e^{-16}$) in comparison with HC. Probabilistic tractography showed fractional anisotropy reduction in the OR in patients with NMOSD-LETM ($p = 0.046$) and NMOSD-ON ($p = 1.50e^{-5}$) compared with HC. Only patients with NMOSD-ON but not NMOSD-LETM showed neuroaxonal damage in the form of pRNFL and GCIPL thinning. VA was normal in patients with NMOSD-LETM and was not associated with OCT or DTI parameters.

Conclusions: Patients with AQP4-ab–seropositive NMOSD without a history of ON have microstructural changes in the afferent visual system. The localization of retinal changes around the Müller-cell rich fovea supports a retinal astrocytopathy. *Neurol Neuroimmunol Neuroinflamm* **2017;4:e334; doi: 10.1212/NXI.0000000000000334**

GLOSSARY

AD = axial diffusivity; **ART** = automatic real time; **DTI** = diffusion tensor imaging; **FT** = foveal thickness; **GCIPL** = ganglion cell and inner plexiform layer; **GEE** = general estimate equation; **HC** = healthy control; **LETM** = longitudinally extensive transverse myelitis; **LGN** = lateral geniculate nucleus; **LPA** = lesion prediction algorithm; **LST** = Lesion Segmentation Toolbox; **MD** = mean diffusivity; **NMOSD** = neuromyelitis optica spectrum disorder; **OCT** = optical coherence tomography; **ON** = optic neuritis; **OR** = optic radiation; **pRNFL** = peripapillary retinal nerve fiber layer; **RD** = radial diffusivity; **ROI** = region of interest; **VA** = visual acuity.

Neuromyelitis optica spectrum disorders (NMOSDs) are relapsing inflammatory conditions of the CNS presenting with optic neuritis (ON) and longitudinally extensive transverse myelitis (LETM) as key clinical features and less frequently brainstem and cerebral involvement.[1] NMOSD is associated with serum antibodies to the astrocytic water channel aquaporin-4 (AQP4), which can be detected in 60%–80% of patients.[2,3] The remainder may not only

---

Table 1   Demographic data of HCs and patients with NMOSD (mean ± SD)

	HC	NMOSD-LETM	NMOSD-ON
Subject, n	26	6	19
Sex, female/male	22/4	6/0	17/2
Age, y	43.6 ± 15.7	43.1 ± 9.83	43.7 ± 12.5
Disease duration, y		3.0 ± 3.7	9.5 ± 8.9
EDSS, median (min–max)		3.5 (1.5–6.5)	4 (0–6)

Abbreviations: EDSS = Expanded Disability Status Scale; HC = healthy control; LETM = longitudinally extensive transverse myelitis; NMOSD = neuromyelitis optica spectrum disorder; NMOSD-LETM = NMOSD patients with a history of LETM but no history of ON; NMOSD-ON = NMOSD patients with a history of ON; ON = optic neuritis.

comprise patients with false-negative AQP4-antibody tests but also true AQP4 seronegatives that may harbor other autoantibodies (e.g., myelin oligodendrocyte glycoprotein) and may thus suffer from distinct disease entities.[4,5]

In contrast to MS, patients with NMOSD virtually never present clinically with progressive disease.[6] However, advanced imaging and histopathologic studies have shown conflicting results as to whether covert tissue damage can occur independent of attack-associated lesions in patients with NMOSD.[7–9] One possible explanation for these discrepancies may be the heterogeneity of previously investigated cohorts comprising both AQP4-antibody (AQP4-ab) positive and negative patients. Also on clinical examination, it may be difficult to identify subtle findings beyond the

overtly affected functional system (i.e., optic nerve or spinal cord).

Against this background, we investigated microstructural and lesion-independent CNS tissue changes in a homogeneous cohort of exclusively AQP4-ab–seropositive NMOSD patients. To exclude any focal attack-related damage, we limited our study to patients who were only presenting with LETM but were otherwise asymptomatic. We used 2 imaging techniques: optical coherence tomography (OCT) to measure retinal thickness and diffusion tensor imaging (DTI)-based probabilistic tractography to analyze the optic radiation (OR).

METHODS **Patients.** We screened 51 patients with NMOSD participating in an ongoing prospective observational cohort study at the NeuroCure Clinical Research Center at the Charité—Universitätsmedizin Berlin. Six patients with a history of LETM but no other attack (i.e., history of ON) (NMOSD-LETM), 19 NMOSD-ON, and 26 age- and sex-matched healthy controls (HCs) were enrolled (table 1). In a previous study including nineteen (76%) of the 25 patients with NMOSD, normal subcortical gray matter volumes and microstructural changes were found.[10] Inclusion criteria were a minimum age of 18 years and a definite diagnosis of AQP4-ab–seropositive NMOSD according to the 2015 International Consensus Diagnostic Criteria.[11] AQP4-ab were determined by a cell-based assay (Euroimmun, Lübeck, Germany). Patients exhibiting ophthalmologic (e.g., glaucoma, myopia >5 dpt) or systemic diseases (e.g., systemic lupus erythematosus), which can potentially influence OCT or DTI results, were excluded from the study (figure 1). Visual function was tested monocularly with habitual correction and under photopic conditions. For high-contrast visual acuity (VA), Early Treatment in Diabetes

Figure 1   Flowchart of cohort selection
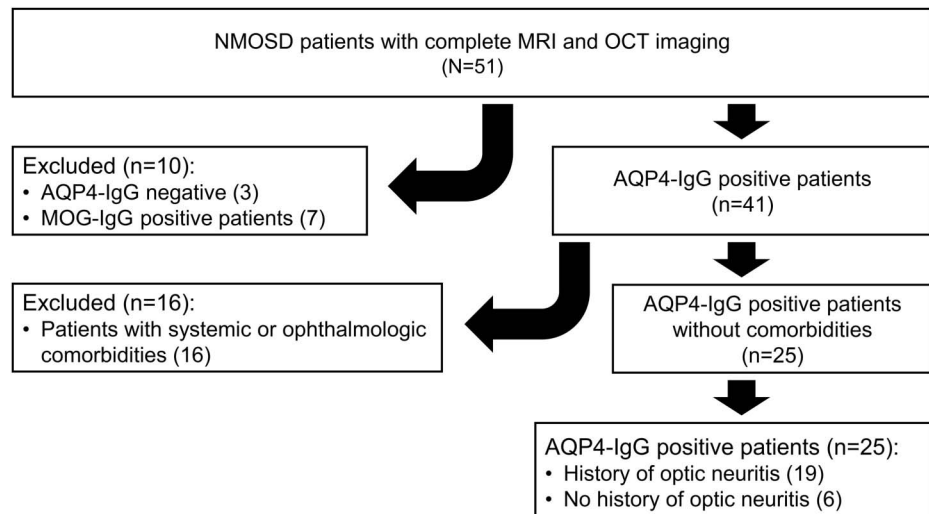
AQP4 = aquaporin-4; MOG = myelin oligodendrocyte glycoprotein; NMOSD = neuromyelitis optica spectrum disorder; OCT = optical coherence tomography.

Retinopathy Study charts were used at a 20-ft distance with an Optec 6500 P system (Stereo Optical, Chicago, IL).[12]

We additionally included a confirmatory OCT cohort consisting of 3 patients with AQP4-ab–seropositive NMOSD-LETM (women/men: 3/0; age: 41.3 ± 10.7 years; disease duration: 2.8 ± 2.1 years), 3 patients with AQP4-ab–seropositive NMOSD-ON (women/men: 3/0; age: 44.0 ± 1.0 years; disease duration: 2.9 ± 0.8 years), and 8 HCs (women/men: 8/0; age: 42.3 ± 1.7 years) following the same inclusion and exclusion criteria from a longitudinal prospective observational cohort study at the Department of Neurology, Klinikum rechts der Isar at the Technical University of Munich, Germany.

Ethics statement. The local ethics committee of the Charité—Universitätsmedizin Berlin approved this study (EA1/131/09). OCT data from the confirmatory cohort were collected under an ethics vote from the ethics committee at the Technical University of Munich (166/16S). The study was conducted in accordance with the Declaration of Helsinki in its currently applicable version and the applicable German laws. All patients provided written informed consent.

Optical coherence tomography. All retinal examinations were performed using a Heidelberg Engineering Spectralis spectral domain OCT (Heidelberg Engineering, Heidelberg, Germany) with automatic real-time (ART) function for image averaging. The peripapillary retinal nerve fiber layer (pRNFL) was measured with activated eye tracker using 3.4-mm ring scans around the optic nerve head (12°, 1,536 A-scans $16 \leq$ ART $\leq$ 100). The combined ganglion cell and inner plexiform layer (GCIPL) volume was measured using a 6-mm diameter cylinder around the fovea from a macular volume scan (25° × 30°, 61 vertical B-scans, 768 A-scans per B-scan, ART = 15).[13] Segmentation of pRNFL and GCIPL was performed semiautomatically using software provided by the OCT manufacturer (Eye Explorer 1.9.10.0 with viewing module 6.0.9.0; Heidelberg Engineering). All measurements were checked for segmentation errors and corrected if necessary by an experienced rater. Foveal thickness (FT) was measured as

the mean thickness of a 1-mm diameter cylinder around the fovea from each collected macular scan. We report our quantitative OCT data in line with the APOSTEL recommendations.[14]

Magnet resonance imaging. All MRI data were acquired on the same 3T scanner (MAGNETOM Trio Siemens, Erlangen, Germany) using a single-shot echo planar, DTI sequence (repetition time [TR]/echo time [TE] = 7,500/86 ms; field-of-view [FOV] = 240 × 240 mm²; matrix 96 × 96, slice thickness 2.3 mm, 64 noncollinear directions, b-value = 1,000 s/mm²), as well as a volumetric high-resolution fluid-attenuated inversion recovery sequence (3D FLAIR) (TR/TE/TI = 6,000/388/2,100 ms; FOV = 256 × 256 mm², slice thickness 1.0 mm). 3D FLAIR images of patients with NMOSD-LETM were checked and verified for OR lesions by a board-certified radiologist. Whole-brain segmentation and quantification of lesions of FLAIR images were performed using lesion prediction algorithm in the Lesion Segmentation Toolbox (LST) for MATLAB 2013a (MathWorks, Inc., Natick, MA).[15]

Probabilistic tractography. Diffusion tensors on the DTI images were fitted by a linear-least square approach. MRtrix package 0.2 (J-D Tournier; Brain Research Institute, Melbourne, Australia) was used to perform probabilistic tractography from seed to target mask.[16] Fiber orientation distribution was estimated with constrained spherical deconvolution and mapped with a maximum harmonic order of 6. The OR reconstruction pipeline was modified from the Martinez-Heras et al.[17] and Lim et al.[18] pipeline. The Juelich probabilistic atlas was used to generate binary masks of lateral geniculate nucleus (LGN) as the seed region of interest (ROI) and primary visual cortex (V1) as the target ROI. For binary exclusion masks, a midline sagittal exclusion plane, a termination coronal plane 20 mm posterior to the temporal pole, and a gray matter segmentation mask were created in the 3D coordinate system of the Montreal Neurological Institute (MNI-152). These were subsequently registered to individual DTI space, serving as a binary exclusion ROI for tractography. Ten thousand

Table 2 OCT and DTI results from HC and NMOSD subgroups (mean ± SD)

	HCs	NMOSD-LETM	NMOSD-ON	NMOSD-LETM vs HC			NMOSD-ON vs LETM			NMOSD-ON vs HC		
				B	SE	p Value	B	SE	p Value	B	SE	p Value
FT, μm	280 ± 21	260 ± 18	262 ± 18	−20.38	8.233	$1.5e^{-2}$	0.952	7.890	$9.0e^{-1}$	−20.32	5.540	$2.4e^{-4}$
pRNFL, μm	97.1 ± 7.4	105.0 ± 6.9	71.7 ± 22.8	−8.28	2.968	$5.3e^{-3}$	−33.03	5.066	$7.0e^{-11}$	−25.6	4.045	$2.4e^{-10}$
GCIPL, mm³	1.87 ± 0.15	1.93 ± 0.11	1.54 ± 0.30	0.061	0.049	$2.1e^{-1}$	−0.389	0.071	$3.9e^{-8}$	−0.333	0.062	$8.3e^{-8}$
FA	0.57 ± 0.04	0.54 ± 0.03	0.53 ± 0.04	−0.029	0.015	$4.6e^{-2}$	−0.014	0.015	$3.2e^{-1}$	−0.046	0.011	$1.5e^{-5}$
MD	0.83 ± 0.07	0.90 ± 0.06	0.87 ± 0.05	0.050	0.032	$1.2e^{-1}$	−0.020	0.026	$4.5e^{-1}$	0.003	0.016	$3.7e^{-2}$
AD	1.43 ± 0.08	1.49 ± 0.09	1.43 ± 0.06	0.044	0.040	$2.7e^{-1}$	−0.048	0.036	$1.8e^{-1}$	−0.003	0.020	$8.7e^{-1}$
RD	0.53 ± 0.08	0.61 ± 0.06	0.59 ± 0.06	0.054	0.031	$8.3e^{-2}$	−0.006	0.026	$8.2e^{-1}$	0.053	0.018	$2.7e^{-3}$
Confirmatory cohort												
FT, μm	286 ± 10	257 ± 4	246 ± 4	−27.89	3.72	$6.6e^{-14}$	−11.36	2.62	$1.4e^{-5}$	−40.62	4.60	$<2.0e^{-16}$
pRNFL, μm	98.2 ± 4.6	114.0 ± 7.2	66.70 ± 14.9	15.68	2.77	$1.5e^{-8}$	−46.51	5.15	$<2.0e^{-16}$	−32.04	4.98	$1.3e^{-10}$
GCIPL, mm³	2.04 ± 0.09	2.07 ± 0.07	1.37 ± 0.14	0.04	0.05	$5.1e^{-1}$	−0.70	0.05	$<2.0e^{-16}$	−0.69	0.03	$<2.0e^{-16}$

Abbreviations: AD = axial diffusivity; B = estimate; FA = fractional anisotropy; FT = foveal thickness; GCIPL = ganglion cell and inner plexiform layer volume; HC = healthy control; LETM = longitudinally extensive transverse myelitis; MD = mean diffusivity; NMOSD = neuromyelitis optica spectrum disorder; NMOSD-LETM = NMOSD patients with a history of LETM but no history of ON; NMOSD-ON = NMOSD patients with a history of ON; OCT = optical coherence tomography; ON = optic neuritis; pRNFL = peripapillary retinal nerve fiber layer thickness; RD = radial diffusivity.

unidirectional streamlines from the LGN to V1 were generated (fractional anisotropy (FA) threshold: 0.1; curvature threshold: 25%; step size: 0.2 mm) for each OR. Streamlines were thresholded for 25% of the maximum value. Resulting fibers were transferred to the Vistalab environment (vistalab.stanford.edu/, Vistalab, Stanford University, Stanford, CA) to compute tract profiles of weighted mean DTI values of FA, mean diffusivity (MD), radial diffusivity (RD), and axial diffusivity at 50 equally spaced positions. We used the middle 30 of the 50 positions for statistical analysis for the exclusion of potential confounders from the LGN to V1 and to have a pure OR volume only.

Statistical analysis. Group differences were tested with a χ^2 test for sex and a Wilcoxon-Mann-Whitney U test for age. Group differences in OCT, DTI, and VA were evaluated by general estimate equation (GEE) models accounting for within-subject intereye dependencies and correcting for age and sex. Relationships between structural and functional parameters were analyzed using GEE models and correcting for age and

sex. Combined p values of exploratory and confirmatory cohort results were calculated by Fisher combined probability test. All tests were performed with R version 3.1.2 with packages psych, geepack, and ggplot2. Graphical representations were created with R and Graphpad Prism 6.0 (Graphpad Software, San Diego, CA). For all calculations, statistical significance was established at $p < 0.05$.

RESULTS OCT analysis. The fovea is a region rich in AQP4-positive Müller cells, and foveal thinning has previously been reported in eyes from patients with NMOSD without ON.[19] We found that FT in eyes from patients with NMOSD-LETM was lower than that in HC, as was FT in patients with NMOSD-ON patients. Remarkably, FT in eyes from patients with NMOSD-LETM never experiencing visual symptoms was comparable to FT in eyes from patients with NMOSD-ON (table 2 and figure 2).

Figure 2   OCT results
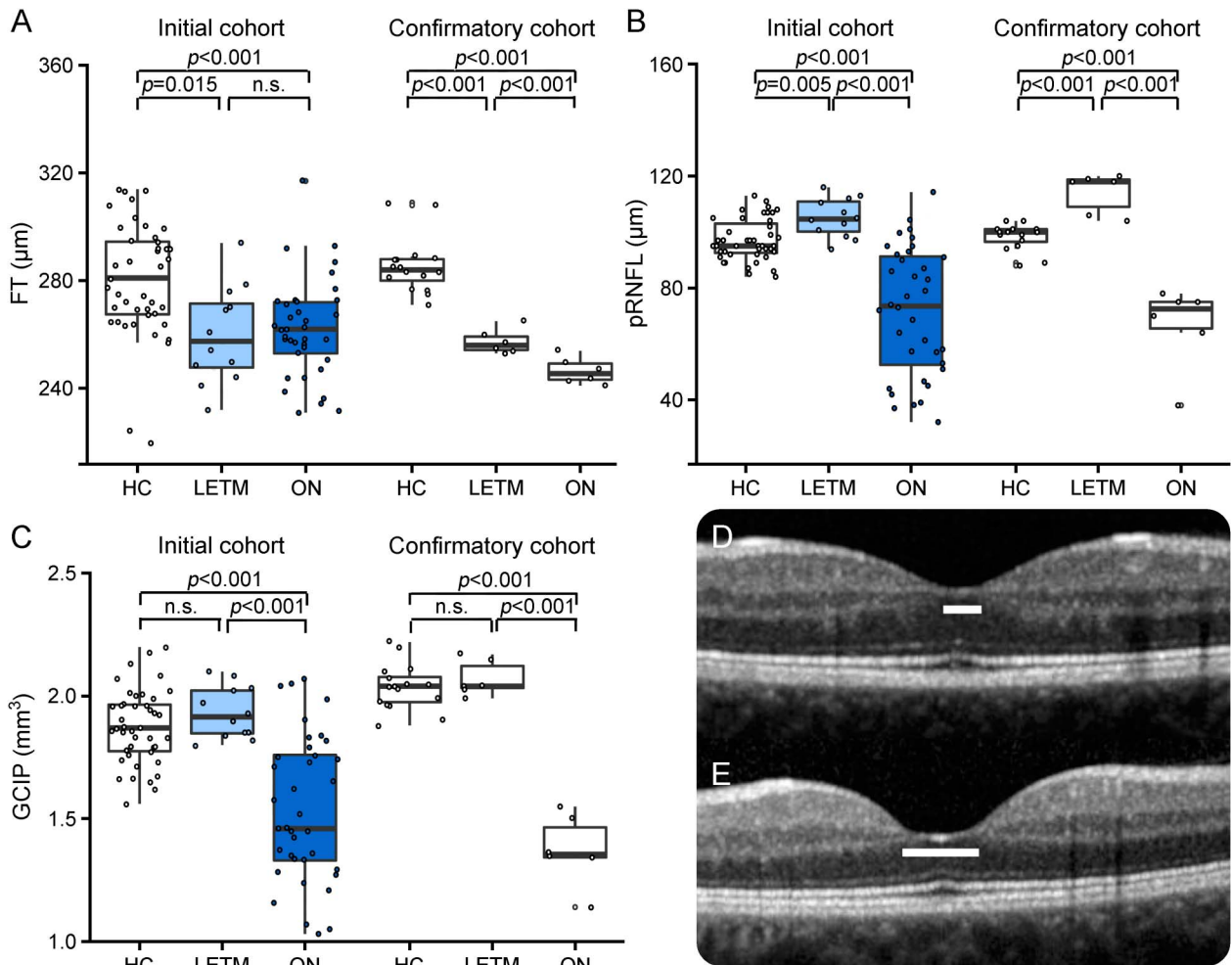
Boxplots of mean OCT values with values of individual eyes (jitter) in HC (left, white), NMOSD-LETM (middle, light blue), NMOSD-ON (right, dark blue), and for each confirmatory cohort (without color) for (A) FT values (μm); (B) pRNFL thickness (μm); (C) GCIPL volume (mm³); (D) FT in a representative macular scan of right eye from an HC; (E) FT changes in a representative macular scan of right eye from a patient with NMOSD-LETM. FT = foveal thickness; GCIPL = combined ganglion cell and inner plexiform layer volume; HC = healthy control; LETM = longitudinally extensive transverse myelitis; NMOSD-LETM = NMOSD patients with a history of LETM but no history of ON; NMOSD-ON = NMOSD patients with a history of ON; OCT = optical coherence tomography; ON = optic neuritis; pRNFL = peripapillary retinal nerve fiber layer thickness.

The FT reduction reflected a change in foveal shape, from an open V-shape in eyes from HCs to a wide U-shape in eyes from patients with NMOSD (figure 2, D–E).

In eyes from patients with NMOSD-LETM, pRNFL and GCIPL as markers of retinal neuroaxonal degeneration were not reduced but pRNFL instead increased in comparison with HC (table 1 and figure 2). By contrast and as expected, eyes with previous ON in the NMOSD-ON group presented with severe pRNFL and GCIPL loss, indicating ON-dependent neuroaxonal damage.[20,21] All OCT results were confirmed in a second independent cohort (figure 2). Statistical combination of p values from the initial and confirmatory cohorts produced immense FT and pRNFL differences between NMOSD-LETM and HC (FT $p = 3.52e^{-14}$, pRNFL $p = 1.93e^{-9}$, and GCIP n.s.) as well as NMOSD-ON and HC (FT $p = 1.24e^{-16}$, pRNFL $p = 1.43e^{-18}$, and GCIP $p = 8.87e^{-22}$), supporting a high likelihood of true-positive results, despite the low sample size in either cohort.

MRI analysis. Microstructural white matter changes in the OR were analyzed using DTI-based probabilistic tractography. Patients with NMOSD-LETM presented with FA reduction in comparison with HC ($p = 0.046$), which suggests structural changes in the OR of patients with NMOSD-LETM (table 2 and figures 3 and 4). Patients with NMOSD-ON expectedly showed pathologic changes in comparison with HCs (FA: $p = 1.5e^{-5}$; MD: $p = 0.037$; and RD: $p = 0.003$).

To ascertain that patients with NMOSD-LETM were indeed asymptomatic with respect to their visual system, we analyzed lesion distribution and volume on brain MRI. Whole-brain lesion volume did not differ between NMOSD-ON (0.95 ± 1.23 mL) and NMOSD-LETM (0.95 ± 1.30 mL; $p > 0.999$). Two patients with NMOSD-LETM had

Figure 3   DTI results 1
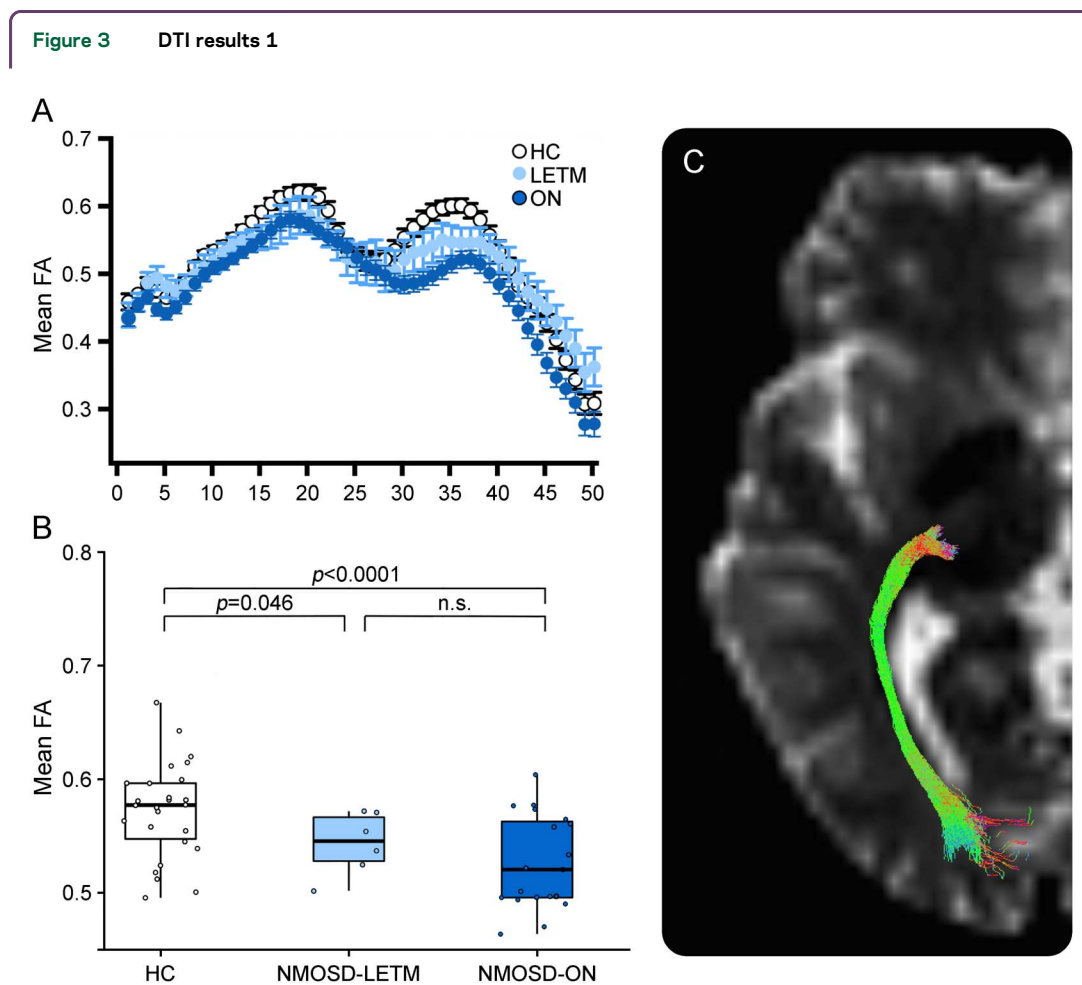
(A) Tract presentation of OR from LGN to V1 for averaged weight-mean DTI values of 50 segments in HC (white), NMOSD-LETM (light blue), and NMOSD-ON (dark blue) for FA (mean ± SEM). (B) Boxplot of mean FA values for middle 3/5 of the OR in HC (left, white), NMOSD-LETM (middle, light blue), and NMOSD-ON (right, dark blue). (C) Example of resulting fibers from tractography analysis. DTI = diffusion tensor imaging; FA = fractional anisotropy; HC = healthy control; LETM = longitudinally extensive transverse myelitis; LGN = lateral geniculate nucleus; NMOSD = neuromyelitis optica spectrum disorder; NMOSD-LETM = NMOSD patients with a history of LETM but no history of ON; NMOSD-ON = NMOSD patients with a history of ON; ON = optic neuritis; OR = optic radiation; V1 = primary visual cortex.

unspecific small dot-like lesions in the OR unilaterally. All confirmatory patients with NMOSD-LETM presented without any lesions in the OR. In patients with NMOSD-LETM, OR FA did not correlate with FT ($r = 0.066$, $p = 0.800$), pRNFL ($r = -0.204$, $p = 0.500$), or GCIPL ($r = 0.261$, $p = 0.400$), suggesting a structurally independent alteration without dependency on the observed foveal changes or covert retinal neuroaxonal damage. In patients with NMOSD-ON, reduced OR FA correlated with

reduced GCIP ($r = 0.361$, $p = 0.030$), but not with FT ($r = 0.210$, $p = 0.200$).

Functional measurements. VA ([logMAR]: -0.02 ± 0.10) was normal in all patients with NMOSD-LETM. As expected, patients with NMOSD-ON had worse mean VA of all eyes ([logMAR]: 0.22 ± 0.37; $p = 0.002$). In patients with NMOSD-LETM and NMOSD-ON, VA did not correlate with FT (NMOSD-LETM: $r = -0.312$, $p = 0.300$;

Figure 4   DTI results 2
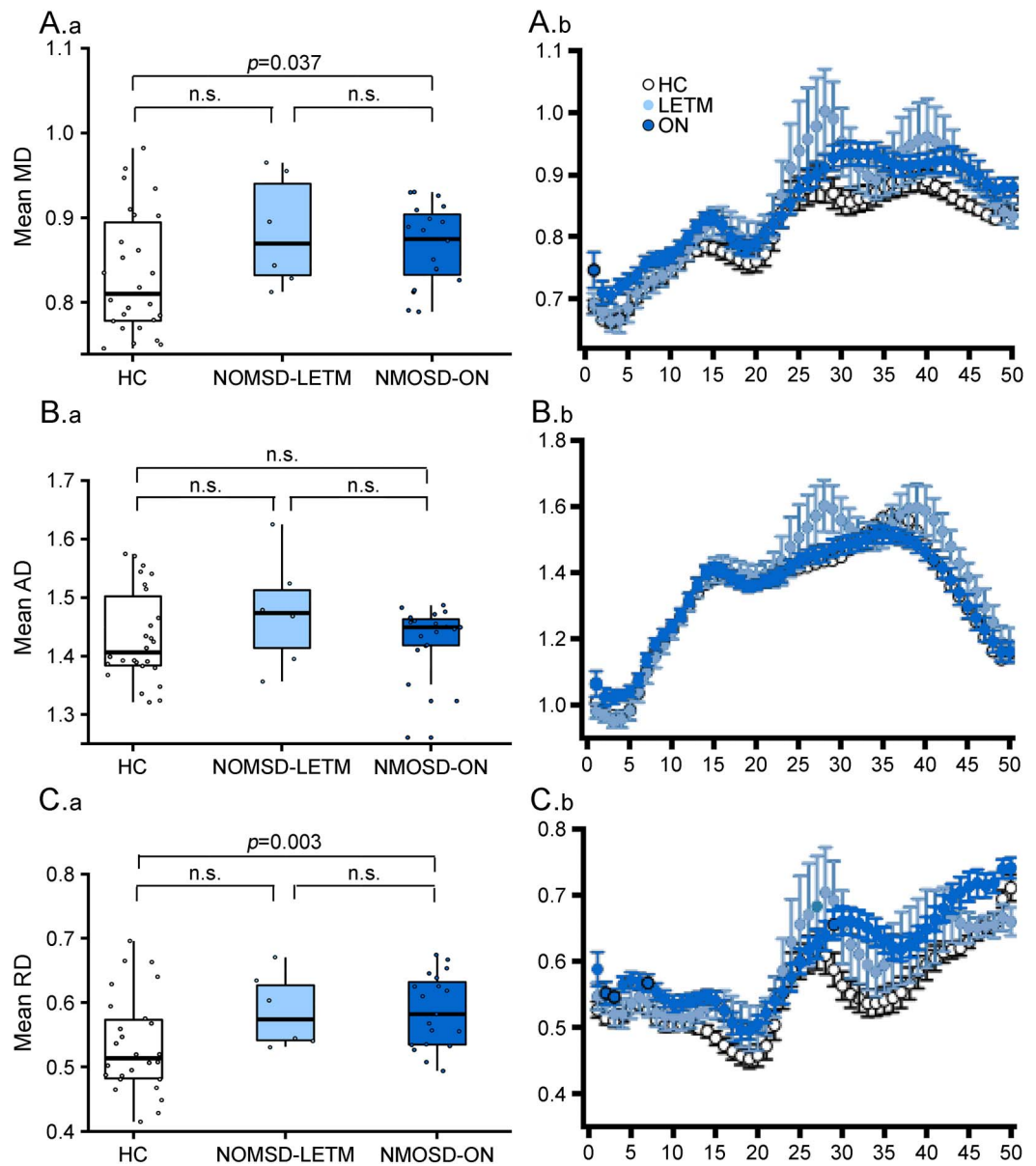
(A.a–C.a) Boxplots of mean DTI values for middle 3/5 of the OR and (A.b–C.b) Tract presentation of OR from the LGN to V1 for averaged weight-mean DTI values of 50 segments in HC (white), NMOSD-LETM (light blue), and NMOSD-ON (dark blue) for (A) MD, (B) AD, and (C) RD (mean ± SEM for all). AD = axial diffusivity; DTI = diffusion tensor imaging; FA = fractional anisotropy; HC = healthy control; LETM = longitudinally extensive transverse myelitis; LGN = lateral geniculate nucleus; MD = mean diffusivity; NMOSD = neuromyelitis optica spectrum disorder; NMOSD-LETM = NMOSD patients with a history of LETM but no history of ON; NMOSD-ON = NMOSD patients with a history of ON; ON = optic neuritis; OR = optic radiation; RD = radial diffusivity; V1 = primary visual cortex.

NMOSD-ON: $r = 0.082$, $p = 0.700$) and OR FA (NMOSD-LETM: VA: $r = -0.445$, $p = 0.100$; NMOSD-ON: $r = 0.073$, $p = 0.700$).

DISCUSSION Patients with AQP4-ab–positive NMOSD without a history of ON and with normal visual function and otherwise normal neuroaxonal retinal measurements (pRNFL, GCIPL) have foveal thinning and reduced OR fractional anisotropy, suggesting microstructural changes in the afferent visual pathway in the absence of clinical attacks of ON.

In NMOSD, 55% of all first clinical events are ONs,[22] which in conjunction with subsequent attacks cause damage to the optic nerve with resultant visual impairment.[20,21,23–25] However, subclinical tissue alterations in NMOSD affecting the afferent visual system have been controversially discussed.[19–21] For example, while one study reported axonal damage in eyes that never experienced ON,[19] another study did not find any signs of neuroaxonal damage in eyes without ON in patients with NMOSD.[21]

Our study now clearly demonstrates structural retinal and OR changes outside attack-related lesions.[26] The parafoveal area is characterized by a high density of retinal astrocytic Müller cells, which express AQP4 and may thus serve as retinal targets in NMOSD.[19,27–29] Müller cells regulate the retinal water balance and have a relevant role in neurotransmitter and photopigment recycling, as well as in energy and lipid metabolism.[27] Müller cell dysfunction or degeneration could thus lead to impaired retinal function including changes in water homeostasis. Of interest, both the initial cohort and the confirmatory cohort showed a mild increase of pRNFL thickness, which could indicate tissue swelling. These findings are supported by animal studies showing retraction of astrocytic end feet in some and astrocyte death in other cases, suggesting a primary astrocytopathy in NMOSD also outside acute lesions.[30–32] The changes we identified in the OR in this study furthermore indicate that a presumptive astrocytopathy may not be confined to the retina.[10,23,25] This is in line with astrocytic end feet changes reported in biopsies from LETM spinal cord lesions and spinal cord atrophy in AQP4-ab–positive patients without previous myelitis.[9,33] Whether these changes lead to subtle clinical manifestations should be further investigated using more sensitive functional measures such as visual evoked potentials or low-contrast VA. If confirmed, this would be in line with a preferential affection of the visual system, even without apparent clinical symptoms in NMOSD.

Reduction of FT in patients with NMOSD without overt clinical evidence of optic nerve involvement (normal VA, normal pRNFL, and GCIPL values) was comparable with that of patients with previous ON. To assure that we were only detecting AQP4-ab–associated pathologies, we rigorously excluded potential confounders. Most importantly, we only included a homogeneous group of AQP4-ab–seropositive patients who are expected to display a well-defined astrocytopathy phenotype.[34] Patients were only eligible if they presented with LETM and no history of ON, visual symptoms, or other typical NMOSD-associated bouts. Since our patients with NMOSD-LETM did not show pRNFL and GCIPL thinning, a previous subclinical ON is highly unlikely. However, a potential pRNFL swelling might have masked a mild subclinical neurodegeneration, but the effects would likely be small and would not be able to explain the observed changes, which are comparable to eyes after severe ON.[21] In light of a recent animal study,[32] it is conceivable that AQP4-specific T cells also contribute to foveal astrocytopathy. However, disease-independent factors in NMOSD, such as prematurity and environmental conditions,[35] may also play a role in foveal thinning.

Previous studies investigating retinal changes in patients with NMOSD regularly included measurements from unaffected fellow eyes from patients with unilateral ON. This is problematic since ON in NMOSD often involves the optic chiasm, and carry-over effects by chiasmic involvement of symptomatically unilateral ON have been reported in up to 64% of patients with AQP4-ab–positive NMOSD.[22] This sets our study apart from a previous study reporting FT reduction in eyes without previous ON in a cohort of patients with NMOSD, which could have been alternatively explained by both non-AQP4 pathologies and chiasmic carry-over effects.[19] Furthermore, none of the patients with NMOSD-LETM had NMOSD-related attacks other than LETM, minimizing the potential of attack- or lesion-related tissue alteration as the cause of the observed changes. Attack-related tissue alteration could have been the case in a recent study reporting spinal cord atrophy in AQP4-ab–positive NMOSD patients with ON.[9] Of interest, despite all patients in the NMOSD-LETM group reporting and showing no symptoms of visual dysfunction, a few patients showed small lesions near the OR. Measurements from these patients were not outliers but well positioned within the data distribution of the whole cohort (not shown).

One important limitation of our study, which we share with the majority of other studies published in NMOSD, is the small sample size. We were able to confirm our results, however, in a second independent cohort. Furthermore, our study cannot answer whether the reported changes are attack related or attack independent (e.g., due to circulating

antibodies). That at least some occult changes might be caused during acute attacks was suggested by a study reporting a correlation of brain volumes and perfusion change with the number of ON attacks in patients with NMOSD.[36]

We found microstructural changes in the afferent visual system in visually asymptomatic patients with AQP4-ab–positive NMOSD-LETM, which were most apparent in the fovea, a region rich in AQP-expressing Müller cells. Localization and extent of these changes are suggestive of an astrocytopathy without apparent neuroaxonal damage. Identifying occult brain changes in patients with NMOSD is important for a number of reasons. These occult changes could be relevant for symptoms that are not directly related to attacks, e.g., cognitive dysfunction, fatigue, and depression[37–39] and could predispose to full attacks causing severe astrocytic damage, demyelination, and neuroaxonal damage. As such, occult CNS including retinal changes in NMOSD may be an important diagnostic and target. Retinal imaging of NMOSD-specific changes could aid in early differential diagnosis of NMOSD and help to identify patients in need of an NMOSD-specific therapy. Although highly specific, antibody testing takes too much time during an initial attack of a de novo NMOSD patient, making acute attack-related therapeutic diversification currently difficult. Future research should thus focus on the sensitivity and specificity of the retinal findings in NMOSD also in contrast to relevant differential diagnoses such as myelin oligodendrocyte glycoprotein antibody (MOG-ab)-associated encephalomyelopathy or MS.[40] Finally, retinal assessment could aid as therapy response marker during novel drug development.

REFERENCES

1. Jarius S, Wildemann B, Paul F. Neuromyelitis optica: clinical features, immunopathogenesis and treatment. Clin Exp Immunol 2014;176:149–164.
2. Metz I, Beißbarth T, Ellenberger D, et al. Serum peptide reactivities may distinguish neuromyelitis optica subgroups and multiple sclerosis. Neurol Neuroimmunol Neuroinflamm 2016;3:e204. doi: 10.1212/NXI.0000000000000204.
3. Zekeridou A, Lennon VA. Aquaporin-4 autoimmunity. Neurol Neuroimmunol Neuroinflamm 2015;2:e110. doi: 10.1212/NXI.0000000000000110.
4. Waters P, Reindl M, Saiz A, et al. Multicentre comparison of a diagnostic assay: aquaporin-4 antibodies in neuromyelitis optica. J Neurol Neurosurg Psychiatry 2016;87:1005–1015.
5. Zamvil SS, Slavin AJ. Does MOG Ig-positive AQP4-seronegative opticospinal inflammatory disease justify a diagnosis of NMO spectrum disorder? Neurol

Neuroimmunol Neuroinflamm 2015;2:e62. doi: 10. 1212/NXI.0000000000000062.

6. Wingerchuk DM, Pittock SJ, Lucchinetti CF, Lennon VA, Weinshenker BG. A secondary progressive clinical course is uncommon in neuromyelitis optica. Neurology 2007;68:603–605.

7. Kremer S, Renard F, Achard S, et al. Use of advanced magnetic resonance imaging techniques in neuromyelitis optica spectrum disorder. JAMA Neurol 2015;72:815–822.

8. Lucchinetti CF, Guo Y, Popescu BFG, Fujihara K, Itoyama Y, Misu T. The pathology of an autoimmune astrocytopathy: lessons learned from neuromyelitis optica. Brain Pathol 2014;24:83–97.

9. Ventura RE, Kister I, Chung S, Babb JS, Shepherd TM. Cervical spinal cord atrophy in NMOSD without a history of myelitis or MRI-visible lesions. Neurol Neuroimmunol Neuroinflamm 2016;3:e224. doi: 10. 1212/NXI.0000000000000224.

10. Finke C, Heine J, Pache F, et al. Normal volumes and microstructural integrity of deep gray matter structures in AQP4+ NMOSD. Neurol Neuroimmunol Neuroinflamm 2016;3:e229. doi: 10.1212/NXI.0000000000000229.

11. Wingerchuk DM, Banwell B, Bennett JL, et al. International consensus diagnostic criteria for neuromyelitis optica spectrum disorders. Neurology 2015;85:177–189.

12. Bock M, Brandt AU, Kuchenbecker J, et al. Impairment of contrast visual acuity as a functional correlate of retinal nerve fibre layer thinning and total macular volume reduction in multiple sclerosis. Br J Ophthalmol 2012;96:62–67.

13. Oberwahrenbrock T, Weinhold M, Mikolajczak J, et al. Reliability of intra-retinal layer thickness estimates. PLoS One 2015;10:e0137316.

14. Cruz-Herranz A, Balk LJ, Oberwahrenbrock T, et al. The APOSTEL recommendations for reporting quantitative optical coherence tomography studies. Neurology 2016; 86:2303–2309.

15. Schmidt P, Gaser C, Arsic M, et al. An automated tool for detection of FLAIR-hyperintense white-matter lesions in multiple sclerosis. Neuroimage 2012;59:3774–3783.

16. Tournier JD, Calamante F, Connelly A. Robust determination of the fibre orientation distribution in diffusion MRI: non-negativity constrained super-resolved spherical deconvolution. Neuroimage 2007;35:1459–1472.

17. Martínez-Heras E, Varriano F, Prčkovska V, et al. Improved framework for tractography reconstruction of the optic radiation. PLoS One 2015;10:e0137064.

18. Lim JC, Phal PM, Desmond PM, et al. Probabilistic MRI tractography of the optic radiation using constrained spherical deconvolution: a feasibility study. PLoS One 2015;10:e0118948.

19. Jeong IH, Kim HJ, Kim NH, Jeong KS, Park CY. Subclinical primary retinal pathology in neuromyelitis optica spectrum disorder. J Neurol 2016;263:1343–1348.

20. Syc SB, Saidha S, Newsome SD, et al. Optical coherence tomography segmentation reveals ganglion cell layer pathology after optic neuritis. Brain 2012;135:521–533.

21. Schneider E, Zimmermann H, Oberwahrenbrock T, et al. Optical coherence tomography reveals distinct patterns of retinal damage in neuromyelitis optica and multiple sclerosis. PLoS One 2013;8:e66151.

22. Ramanathan S, Prelog K, Barnes EH, et al. Radiological differentiation of optic neuritis with myelin oligodendrocyte glycoprotein antibodies, aquaporin-4 antibodies, and multiple sclerosis. Mult Scler J 2016;22:470–482.

23. Pache F, Zimmermann H, Finke C, et al. Brain parenchymal damage in neuromyelitis optica spectrum disorder: a multimodal MRI study. Eur Radiol 2016;26:4413–4422.

24. Rueda Lopes FC, Doring T, Martins C, et al. The role of demyelination in neuromyelitis optica damage: diffusion-tensor MR imaging study. Radiology 2012;263:235–242.

25. Zhao DD, Zhou HY, Wu QZ, et al. Diffusion tensor imaging characterization of occult brain damage in relapsing neuromyelitis optica using 3.0T magnetic resonance imaging techniques. Neuroimage 2012;59:3173–3177.

26. Kim HJ, Paul F, Lana-Peixoto MA, et al. MRI characteristics of neuromyelitis optica spectrum disorder: an international update. Neurology 2015;84:1165–1173.

27. Reichenbach A, Bringmann A. Müller Cells in the Healthy and Diseased Retina. New York: Springer; 2010.

28. Nicchia GP, Pisani F, Simone L, et al. Glio-vascular modifications caused by Aquaporin-4 deletion in the mouse retina. Exp Eye Res 2016;146:259–268.

29. Felix CM, Levin MH, Verkman AS. Complement-independent retinal pathology produced by intravitreal injection of neuromyelitis optica immunoglobulin G. J Neuroinflammation 2016;13:275.

30. Kurosawa K, Misu T, Takai Y, et al. Severely exacerbated neuromyelitis optica rat model with extensive astrocytopathy by high affinity anti-aquaporin-4 monoclonal antibody. Acta Neuropathol Commun 2015;3:82.

31. Misu T, Fujihara K, Kakita A, et al. Loss of aquaporin 4 in lesions of neuromyelitis optica: distinction from multiple sclerosis. Brain 2007;130:1224–1234.

32. Zeka B, Hastermann M, Kaufmann N, et al. Aquaporin 4-specific T cells and NMO-IgG cause primary retinal damage in experimental NMO/SD. Acta Neuropathol Commun 2016;4:82.

33. Hayashida S, Masaki K, Yonekawa T, et al. Early and extensive spinal white matter involvement in neuromyelitis optica. Brain Pathol Epub 2016 Apr 15.

34. Hinson SR, Pittock SJ, Lucchinetti CF, et al. Pathogenic potential of IgG binding to water channel extracellular domain in neuromyelitis optica. Neurology 2007;69: 2221–2231.

35. Provis JM, Dubis AM, Maddess T, Carroll J. Adaptation of the central retina for high acuity vision: cones, the fovea and the avascular zone. Prog Retin Eye Res 2013;35:63–81.

36. Sánchez-Catasús CA, Cabrera-Gomez J, Almaguer Melián W, et al. Brain tissue volumes and perfusion change with the number of optic neuritis attacks in relapsing neuromyelitis optica: a voxel-based correlation study. PLoS One 2013;8:e66271.

37. Liu Y, Duan Y, He Y, et al. A tract-based diffusion study of cerebral white matter in neuromyelitis optica reveals widespread pathological alterations. Mult Scler J 2012; 18:1013–1021.

38. Finke C, Schlichting J, Papazoglou S, et al. Altered basal ganglia functional connectivity in multiple sclerosis patients with fatigue. Mult Scler J 2015;21:925–934.

39. Chavarro VS, Mealy MA, Simpson A, et al. Insufficient treatment of severe depression in neuromyelitis optica spectrum disorder. Neurol Neuroimmunol Neuroinflamm 2016;3:e286. doi: 10.1212/NXI.0000000000000286.

40. Pache F, Zimmermann H, Mikolajczak J, et al. MOG-IgG in NMO and related disorders: a multicenter study of 50 patients: part 4: afferent visual system damage after optic neuritis in MOG-IgG-seropositive versus AQP4-IgG-seropositive patients. J Neuroinflammation 2016;13:282.

Neurology®
Neuroimmunology
& Neuroinflammation

This information is current as of February 22, 2017

Updated Information & Services	including high resolution figures, can be found at: http://nn.neurology.org/content/4/3/e334.full.html
References	This article cites 38 articles, 7 of which you can access for free at: http://nn.neurology.org/content/4/3/e334.full.html##ref-list-1
Subspecialty Collections	This article, along with others on similar topics, appears in the following collection(s): **Devic's syndrome** http://nn.neurology.org//cgi/collection/devics_syndrome **DWI** http://nn.neurology.org//cgi/collection/dwi **Retina** http://nn.neurology.org//cgi/collection/retina
Permissions & Licensing	Information about reproducing this article in parts (figures,tables) or in its entirety can be found online at: http://nn.neurology.org/misc/about.xhtml#permissions
Reprints	Information about ordering reprints can be found online: http://nn.neurology.org/misc/addir.xhtml#reprintsus

AMERICAN ACADEMY OF
NEUROLOGY®